Antiferromagnetic coupling between the Mn and Fe nearest neighbours in ferromagnetic Mn:Pt-10 at.% Fe

1992 J. Phys.: Condens. Matter 4 9181

(http://iopscience.iop.org/0953-8984/4/46/021)

J. Phys.: Condens. Matter 4 (1992) 9181–9190. Printed in the UK

Antiferromagnetic coupling between the Mn and Fe nearest neighbours in ferromagnetic Mn:Pt–10 at.% Fe

M Trhlík†‡¶, P De Moor†, A L Erzinkyan§, G M Gurevich||, V P Parfenova§, P Schuurmans†, N Severijns†, W Vanderpoorten†, L Vanneste† and J Wouters†

† Instituut voor Kern-en Stralingsfysika, Katholieke Universiteit, Celestijnenlaan 200D, B-3030 Leuven, Belgium

‡ Department of Low-Temperature Physics, Charles University, V Holešovičkách 2, 18 000 Prague 8, Czechoslovakia

§ Institute of Nuclear Physics, Moscow State University, 177234 Moscow, Russia

|| Institute for Nuclear Research, Russian Academy of Sciences, 177312 Moscow, Russia

Received 27 May 1992

Abstract. The low-temperature nuclear orientation of ^{54}Mn in ferromagnetic Pt–10 at.% Fe has been studied in the temperature range 4–50 mK and in the external magnetic field range 0.5–8.5 T. Considerable non-collinearity of Mn magnetic moments with respect to the bulk magnetization direction has been found in the whole B_{ext} range. A model based on the Heisenberg Hamiltonian in the first-neighbour approximation is proposed, which fully describes our experimental data. We found that the first-neighbour Mn–Fe exchange interaction is antiferromagnetic with the value $J_{Mn-Fe} = -21(1)$ K, which lies in the range of the nearest-neighbour Mn–Mn or Fe–Fe exchange interaction parameters for Pt-based alloys.

1. Introduction

Pt–Fe alloys are systems with magnetic clusters localized around Fe atoms and they show ferromagnetic order above 0.76 at.% Fe [1]. The magnetic behaviour of these alloys has been successfully described by the magnetic environment model [2, 3]. Neutron diffraction experiments on Pt–10 at.% Fe have resulted in average magnetic moments localized on Fe and Pt atoms given by $\mu_{Fe} = 3.12(2)\mu_B$ and $\mu_{Pt} = 0.198(2)\mu_B$, respectively [4], and $T_C = 160$ K [5, 6]. A study of the critical parameters has shown that this alloy belongs to the universal class of 3D Heisenberg magnets [6]. At higher Fe concentrations the magnetic structure of Pt–Fe alloys is more complicated. The disordered Pt_3Fe alloy is a ferromagnet, unlike the ordered Pt_3Fe system, which is an antiferromagnet with $T_N = 170$ K [7].

Unlike Fe impurities, Mn impurities in Pt polarize the surrounding Pt atoms only weakly and the magnetic moment of a cluster around an Mn impurity for Pt–5 at.% Mn ($\mu_{cl} = 5.5\mu_B$) [8] does not much exceed the Mn free-spin value ($\mu_{Mn} = 5\mu_B$). The spin-glass state has been observed in Pt–Mn in the concentration range 0.05–3.8 at.% Mn [9, 10]; this is attributed to the antiferromagnetic coupling between

¶ Present and permanent address: Department of Low-Temperature Physics, Charles University, V Holešovičkách 2, 180 00 Prague 8, Czechoslovakia.

0953-8984/92/469181+10$07.50

neighbouring Mn–Mn pairs. On the other hand, the ordered Pt_3Mn system is a ferromagnet with $T_C = 390$ K and with magnetic moments localized on both Mn and Pt sites [11].

The low-temperature nuclear orientation (NO) technique is a useful tool for studying local magnetic structure around an impurity (see the recent review in [12]). In NO experiments the angular distribution $W(\theta, T)$ of γ-rays of radioactive probe nuclei at sufficiently low temperature T is measured. For our ^{54}Mn probe the anisotropy $W(\theta, T)$ can be expressed by the formula

$$W(\theta, T) = 1 + Q_2 A_2 B_2(E_m/kT) P_2(\cos\theta) + Q_4 A_4 B_4(E_m/kT) P_4(\cos\theta) \qquad (1)$$

where Q_k and $A_k(B_k)$ are the known constants (functions) conventionally defined in the literature on NO (e.g. [12]). E_m is the hyperfine splitting energy defined by

$$E_m = g_N \mu_N B_{tot} \qquad (2)$$

with

$$\boldsymbol{B}_{tot} = \boldsymbol{B}_{hf} + \boldsymbol{B}_{ext} \qquad (3)$$

where $\boldsymbol{B}_{tot}$ is the total magnetic field acting on the nuclei. $\boldsymbol{B}_{hf}$ and $\boldsymbol{B}_{ext}$ are the hyperfine and external magnetic fields, respectively. The functions P_k are the Legendre polynomials and θ is the angle between $\boldsymbol{B}_{tot}$ and the γ-ray observation direction.

Using NO, Thompson *et al* [13] have investigated the behaviour of Mn spins in pure Pt and have found that the Mn magnetization deviates from purely paramagnetic behaviour at very low B_{ext}, probably owing to Mn interactions with one or more other 3D impurities of very low concentrations in the host. In our earlier papers [14, 15] we reported the NO study of ^{54}Mn impurities in low-Fe-concentration (0.05–1 at.%) Pt–Fe alloys. Considerable non-collinearity of Mn magnetic moments with respect to the matrix magnetization has been found at external fields of several teslas. In the case of ferromagnetic Pt–1 at.% Fe the Mn magnetic moment saturation was not achieved even when $B_{ext} = 9$ T. The study of ^{54}Mn in ferromagnetic Pt–10 at.% Fe at lower B_{ext} [16] has shown that the Mn spins are frozen with a mean angle of about 20° with respect to the matrix magnetization. B_{ext}-values from 0.4 to 1.2 T have no effect on this Mn misalignment.

In this paper we present an NO experimental study of ^{54}Mn:Pt–10 at.% Fe in the temperature range 4–50 mK and the B_{ext} range 0.5–8.5 T. A simple model based on the localized spin model with the first-neighbour interaction approximation, which completely described our experimental data, has been proposed. The value obtained for the Mn–Fe exchange parameter is discussed.

2. Experiment

The sample ^{54}Mn:Pt–10 at.% Fe was prepared by the standard melting technique followed by cold rolling and annealing in high vacuum and was the same as used in [16]. The total Mn concentration in the sample (including non-active Mn) was

estimated to be below 10 ppm. The sample in the form of a foil was soldered to the cold finger of the dilution refrigerator with its surface parallel to the B_{ext} direction.

The NO experiments were performed at the off-line NO facility at Leuven in the B_{ext} range 0.5–8.5 T and in the temperature range 4–50 mK (the temperature even fell to 3 mK when B_{ext} was reduced very slowly to between 1 and 2 T, probably as a result of nuclear demagnetization of the copper finger). A ^{57}Co–Fe NO thermometer and a Ge(Li) detector in the B_{ext} direction were used.

Experimental values of the anisotropy W as a function of both temperature and B_{ext} have been obtained. The temperature dependences of W for four B_{ext}-values are shown in figures 1 and 2.

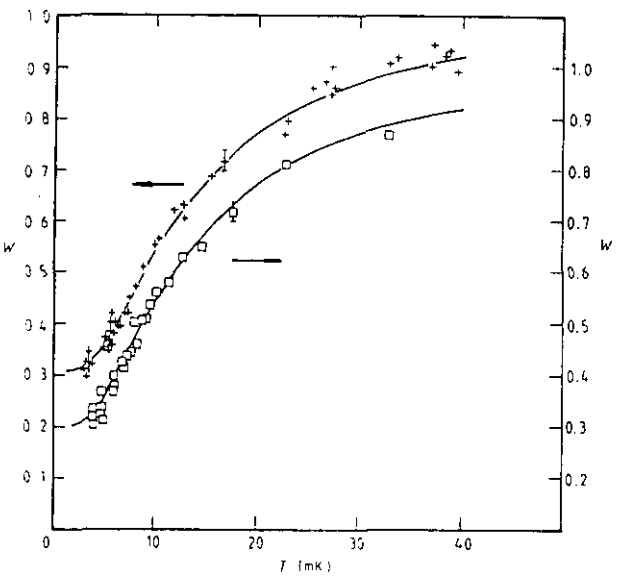

Figure 1. The temperature dependence of W for ^{54}Mn:Pt–10 at.% Fe: +, experimental values, $B_{ext} = 2$ T; □, experimental values, $B_{ext} = 4$ T; ——, best fit (see text).

3. Analyses of the experimental data and discussion

3.1. Fictitious hyperfine field

The most straightforward analysis of the experimental W data is based on the assumption that only one 'effective' hyperfine field B_{eff} acts on the ^{54}Mn nuclei, which is collinear with B_{ext} and negative (by analogy to B_{hf} on ^{54}Mn in pure Pt (i.e. −36.5(15) T) [13]). Thus, using (1)–(3) and supposing that $\theta = 0°$, one can calculate these fictitious B_{eff}-values from the experimental anisotropies W. The temperature dependences of B_{eff} for three B_{ext}-values are shown in figure 3.

As one can see from our data, there is a significant temperature dependence of B_{eff} even when $B_{ext} = 8.5$ T. B_{eff} also depends on B_{ext} when the temperature is constant. On the other hand, at higher temperatures and B_{ext}-values the B_{eff}-values tend to 'saturate' at a value which is close to the B_{hf}-value of ^{54}Mn in Pt.

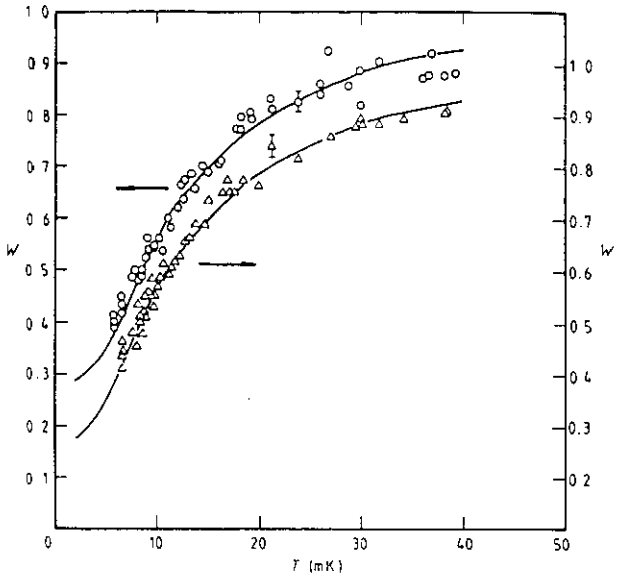

Figure 2. The temperature dependence of W for ^{54}Mn:Pt–10 at.% Fe: ○, experimental values, $B_{ext} = 7$ T; △, experimental values, $B_{ext} = 8.5$ T; ——, best fit (see text).

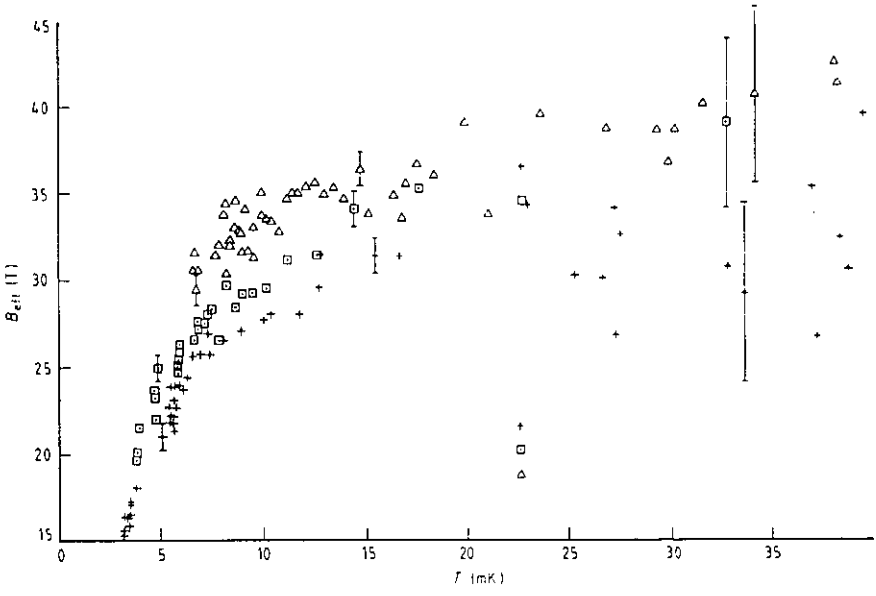

Figure 3. The temperature dependence of the effective field B_{eff} on ^{54}Mn in Pt–10 at.% Fe: +, $B_{ext} = 2$ T; □, $B_{ext} = 4$ T; △, $B_{ext} = 8.5$ T.

The strong temperature dependence of B_{eff} indicates that the extraction of B_{eff} from W using (1)–(3) with $\theta = 0°$ is not correct. In order to obtain a true value of B_{hf}, some non-collinearity of B_{hf} with respect to B_{ext} ($\theta = 0°$) must be assumed (see, e.g., [14, 17]).

3.2. Non-collinearity of Mn magnetic moments

As a more realistic model we assumed that there was some non-collinearity between $\boldsymbol{B}_{ext}$ (which is in the γ-ray observation direction) and the Mn magnetic moment (which is in the $\boldsymbol{B}_{hf}$ direction). We fitted the temperature dependence of W at a given B_{ext}(= 0.5, 2, 4, 5.5, 7 and 8.5 T) using (1)–(3) with two free parameters: a B_{hf}-value and an angle α between $\boldsymbol{B}_{hf}$ and $\boldsymbol{B}_{ext}$. The fits resulted in χ^2-values of approximately unity and B_{hf}-values near the B_{hf} for pure Pt (our mean value $B_{hf} = (-)38(2)$ T). The angle α decreased when B_{ext} increased (from $\alpha = 18.8(3)°$ at $B_{ext} = 0.5$ T to $\alpha = 15.6(2)°$ at $B_{ext} = 8.5$ T).

As a next step we recalculated all W-values for $\cos\alpha$ using (1)–(3) and assuming $B_{hf} = (-)38$ T. The B_{ext} dependence of $\cos\alpha$ for the temperature range 3–10 mK is shown in figure 4. If we suppose that $\mu_{Mn} \propto B_{hf}$, we can conclude that the Mn magnetic moment in Pt–10 at.% Fe preserves its free-spin value but it is not aligned along B_{ext} even at higher B_{ext}. B_{ext} turns it only slightly.

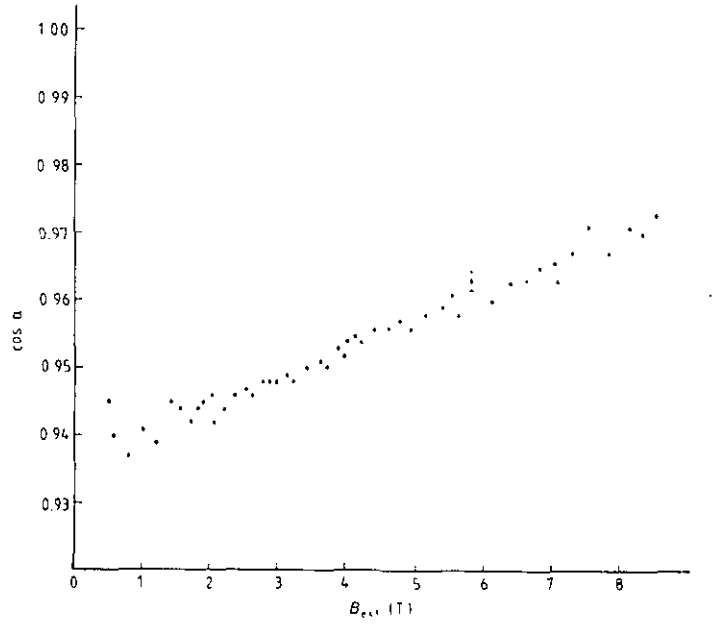

Figure 4. The B_{ext} dependence of $\cos\alpha$ (α is the angle of non-collinearity) for ^{54}Mn:Pt–10 at.% Fe (T = 3–10 mK).

As a reason for the observed Mn non-collinearity, a misalignment of the matrix itself cannot be completely excluded. In principle, competition between ferromagnetic and antiferromagnetic coupling between both Fe spins and/or Fe–Pt clusters could lead to asperomagnetic behaviour (see, e.g., [18]). The magnetic measurements of Pt–1 at.% Fe [19] demonstrated that this alloy does not show perfect ferromagnetic order. Hamzic *et al* [20] claim that the ferromagnetic alloys Pt–Fe (1–5 at.% Fe) are not perfectly aligned even when $B_{ext} \simeq 3$ T and the temperature is much less than T_C, probably because of a partially unquenched Fe orbital moment [21]. On the

other hand, our latest Mössbauer study of Pt–10 at.% Fe at 4.2 K [22] has shown the complete alignment of Fe spins at $B_{ext} \geqslant 0.5$ T. We therefore believe that our higher-Fe-concentration Pt–Fe matrix has the Fe (and Pt) spins completely aligned along B_{ext} even at lower B_{ext} in the temperature range used.

The Mn spin (probably including its nearest neighbours) is therefore misaligned with respect to the matrix magnetization. Since the Mn orbital moment is completely quenched in Pt [21] and the Mn–Mn interactions can be neglected owing to a very low Mn concentration, the most probable reason for this behaviour is antiferromagnetic coupling of Mn spins with some surrounding spins. Because of the variety of Mn nearest neighbours, our assumption that the only misalignment angle is α seems to be too simple.

3.3. Localized-spin model

For a deeper understanding of the observed Mn behaviour the following model, based on the localized-spin model, has been proposed. We used the following assumptions.

(a) The magnetic moments are localized on the Pt, Fe and Mn sites with the values $\mu_{Pt} = 0.2\mu_B$, $\mu_{Fe} = 3.12\mu_B$ [4] and $\mu_{Mn} = 5\mu_B$ (we assume the Mn free-spin value). The system is described by the Heisenberg Hamiltonian

$$H = \sum_{i,j} J_{ij} S_i S_j \tag{4}$$

where J_{ij} is the exchange interaction parameter between the ith and jth atoms and $S_i = \mu_i/2\mu_B$. Hereafter we take into account the nearest-neighbour interaction only.

(b) The Fe and Mn atoms are randomly distributed in the Pt FCC lattice. The probability p_n that the Mn atom has n Fe atoms as its first neighbours is given by the binomial law

$$p_n = \binom{12}{n} (1 - c_{Fe})^{12-n} c_{Fe}^n \tag{5}$$

where c_{Fe} is the Fe atomic concentration (we assume that $c_{Mn} \to 0$). In our case for $c_{Fe} = 0.1$ we obtain $p_0 = 0.282$, $p_1 = 0.377$, $p_2 = 0.230$, $p_3 = 0.085$, etc.

(c) The Fe spin feels the influence of B_{ext} and the molecular field B_{mol}^{Fe}. In the molecular-field approximation, B_{mol}^{Fe} can be estimated as

$$B_{mol}^{Fe} = 3T_C k/2\mu_B(S_{Fe} + 1). \tag{6}$$

For our case ($T_C = 160$ K [6]), $B_{mol}^{Fe} = 140$ T. Similar influences of B_{ext} and B_{mol}^{Mn} on the Mn spin can be considered except that B_{mol}^{Mn} is unknown.

As we pointed out earlier, we are taking into account only the nearest-neighbour interactions which are the following:

(1) the exchange Mn–Fe interaction

$$E_{ex} = -J_{Mn-Fe} S_{Mn} S_{Fe} \qquad \text{(probably } J_{Mn-Fe} < 0\text{)}$$

(2) the interaction of Fe and Mn moments with the external magnetic field and the molecular field (in the classical limit)

$$E_{f,m} = -2\mu_B S_{f,m}\left\{B_{ext} + [(12 - n_{m,f})/12]B_{mol}^{f,m}\right\}$$

where the subscripts f and m correspond to Fe and Mn atoms, respectively.

Thus the energy for an 'Mn site' (Mn atom plus its first neighbours) can be presented in the form

$$E_n = A_n \cos\alpha + C_n \cos\beta + D_n \cos(\alpha - \beta) \tag{7}$$

where $A_n = E_{Mn}$, $C_n = nE_{Fe}$, $D_n = nE_{ex}$, $n = n_{Fe}$ is the number of Fe atoms as first neighbours ($n_{Mn} = 1$ since $c_{Mn} \to 0$), and α and β are the angles between B_{ext} and the Mn and Fe magnetic moments, respectively (we assume that $B_{ext} \| B_{mol}$).

The interaction of Mn and Fe with the Pt atoms does not appear in (7) directly as it is taken into account through B_{mol}.

For our temperature range, α and β are obtained by the minimization (7). The results for $\cos\alpha_n$, which is of interest, are firstly, for the weak antiferromagnetic or ferromagnetic Mn–Fe exchange interaction,

$$\begin{aligned} &D_n \leqslant -A_n C_n/(A_n + C_n) \\ &\cos\alpha_n = +1 \end{aligned} \tag{8}$$

secondly, for the intermediate antiferromagnetic Mn–Fe exchange interaction,

$$\begin{aligned} &+(A_n C_n)/|A_n - C_n| \geqslant D_n \geqslant -A_n C_n/(A_n + C_n) \\ &\cos\alpha_n = [D_n^2(C_n^2 - A_n^2) - A_n^2 C_n^2]/2A_n^2 C_n D_n \end{aligned} \tag{9}$$

and thirdly, for the strong antiferromagnetic Mn–Fe exchange interaction,

$$\begin{aligned} &D_n \geqslant +A_n C_n/|A_n - C_n| \\ &A_n > C_n : \cos\alpha_n = -1 \\ &A_n < C_n : \cos\alpha_n = +1. \end{aligned} \tag{10}$$

The anisotropy W is then given by

$$W = \sum_{n=0}^{12} p_n W'(\cos\alpha_n) \tag{11}$$

where W' is calculated from (1)–(3) and (8)–(10) considering that both B_{tot} and $\cos\theta$ are functions of B_{hf} and $\cos\alpha_n$.

We have carried out the fit using (11) to all our $W(T, B_{ext})$ data with three free parameters: B_{hf}, B_{mol}^{Mn} and J_{Mn-Fe}. The best-fit values are

$$\begin{aligned} &B_{hf} = (-)40(1)\,\mathrm{T} \\ &B_{mol}^{Mn} = +64(4)\,\mathrm{T} \\ &J_{Mn-Fe} = -21(1)\,\mathrm{K} \end{aligned} \tag{12}$$

with $\chi^2 \simeq 1$. As an example of the good correspondence between the model with the best-fit values and our experiment the fitted curves are shown in figures 1 and 2.

The B_{hf} obtained is close to the hyperfine field on ^{54}Mn in Pt (= −36.5(15) T [13]) and also to that on ^{54}Mn in pure Pd (= −38 T [23]), where the Mn free-spin value is supposed. We can conclude that in the ferromagnetic Pt–10 at.% Fe alloy the Mn magnetic moment also holds its free-spin value of about $5\mu_B$, as we assumed.

3.4. Exchange interaction parameters

Some parameters of the exchange interaction between Mn and Fe spins in Pt-based alloys, which are available from the literature, are summarized in table 1.

Table 1. Parameters of the exchange interaction between Mn and Fe spins in Pt-based alloys.

Exchange interaction	Mutual distance (lattice parameter)	Matrix	J (K)	Reference	Remarks
Fe–Fe	1	Pt_3Fe	+34	[24]	Neutron diffraction, six-exchange-parameter fit
	$\sqrt{2}$		−20		
	$\sqrt{3}$		+16		
Mn–Mn	1	Pt_3Mn	+45	[11]	From T_C, only the first-neighbour Mn–Mn interaction assumed ($S \simeq 2.5$)
Mn–Mn	$1/\sqrt{2}$	$PtMn_3$	−44	[25]	From T_N, $J_2 \simeq 0$, $S \simeq 2.5$
Mn–Fe	$1/\sqrt{2}$	Mn:Pt–10 at.% Fe	−21	This work	See text

The Fe–Fe exchange interactions in ordered Pt_3Fe [24] show an oscillatory character of the RKKY type. The exchange parameter of the Fe–Fe interaction in Pt (mutual Fe–Fe distance $1/\sqrt{2}$) is not definitely known, but antiferromagnetic coupling is not completely excluded. The ferromagnetic behaviour of the low-Fe-concentration Pt–Fe alloys could then be caused by the large ferromagnetic-type Pt–Pt and Fe–Pt interactions, as was assumed in [2, 3].

The Mn–Mn exchange interactions in Pt-based alloys seem to be of the RKKY type too with the first-neighbour interaction being antiferromagnetic. This is probably the reason that the low-Mn-concentration Pt–Mn alloys are spin-glass systems, since the ferromagnetic Mn–Pt interaction is much weaker than the Fe–Pt interaction.

The oscillatory character of Mn–Mn interactions has also been found in low-Mn-concentration Pd–Mn alloys [26]. The exchange interaction between the nearest-neighbour Mn atoms has been estimated to be antiferromagnetic with $J \simeq -9$ K.

In the light of these facts our result—the antiferromagnetic exchange interaction between the Mn and Fe first neighbours in Pt—is quite reasonable. Even its magnitude lies in the range of the exchange interaction parameter values in similar materials.

The value of B_{mol}^{Mn} is somewhat lower than B_{mol}^{Fe} for our alloy; this could be connected with the lower ability of the Mn spins to polarize surrounding Pt atoms. On the other hand, when the value of J_{Mn-Pt} is calculated and then, using the model

proposed for Pt–Fe [2], the magnitude of the magnetic moment of a cluster around an Mn atom in dilute Pt–Mn is derived, one obtains an unrealistically large value (about $20\mu_B$). This contradicts the experimental value (about $5.5\mu_B$) [9, 10]. This indicates that our B_{mol}^{Mn}-value is caused not only by the Pt first neighbours but also, as in the case of B_{mol}^{Fe}, by the next Fe atoms, which can contribute ferromagnetically. Our model should therefore be considered as oversimplified, especially because of the first-neighbour approximation.

4. Conclusions

Considerable non-collinearity of Mn spins with respect to the bulk magnetization in the ferromagnetic alloy Pt–10 at.% Fe has been found at low temepratures and high B_{ext} using the NO technique. The simple model based on the Heisenberg Hamiltonian in the first-neighbour approximation has described our experimental data. The Mn–Fe first-neighbour exchange interaction has been determined as antiferromagnetic, with the magnitude being in the range of the similar Mn–Mn and Fe–Fe exchange interactions in the Pt-based alloys.

The model proposed has shown how to interpret similar NO experiments. We believe that the NO technique could thus be used to obtain information about unknown exchange interaction parameters in suitable magnetic systems.

Acknowledgments

The authors thank Professor B Sedlák for fruitful discussions and Mr P Schoovaerts for technical assistance during the experiment. One of the authors (MT) would like to thank the staff of the Instituut voor Kern-en Stralingsfysika, Katholieke Universiteit Leuven, for hospitality and the Academic Board of the Catholic University of Leuven for the award of a Fellowship.

References

[1] Ododo J C 1979 *J. Phys. F: Met. Phys.* **9** 1441–9
[2] Gonzáles A C and Parra R 1984 *J. Appl. Phys.* **55** 2045–7
[3] Medina R, Parra R E, Mora G and Gonzáles A C 1985 *Phys. Rev.* B **32** 1628–31
[4] Ododo J C 1982 *J. Phys. F: Met. Phys.* **12** 1821–40
[5] Segnan R 1967 *Phys. Rev.* **160** 404–8
[6] Radhakrishna P, Gilder H M, Parette G and Menelle A 1989 *Phys. Rev.* B **40** 2435–41
[7] Bacon G E and Crangle J 1963 *Proc. R. Soc.* A **272** 387–402
[8] Tholence J L and Wassermann E F 1977 *Physica* B **86–8** 875–6
[9] Kästner J, Wassermann E F, Matho K and Tholence J L 1978 *J. Phys. F: Met. Phys.* **8** 103–15
[10] Kiymac K and Finn C B P 1982 *J. Phys. F: Met. Phys.* **12** 333–49
[11] Antonini B, Lucari F, Menzinger F and Paoletti A 1969 *Phys. Rev.* **187** 611–8
[12] Brewer W D 1990 *Rep. Prog. Phys.* **53** 483–548
[13] Thompson J R, Thomson J O, Huray P G, Nave S and Nichols T L 1978 *J. Phys. F: Met. Phys.* **8** 169–75
[14] Trhlík M, Sedlák B, Erzinkyan A L, Gurevich G M, Parfenova V P, Topalov S V, Malinský P and Pavlov V N 1988 *J. Phys. F: Met. Phys.* **18** L237–40
[15] Trhlík M, Dupák J, Sedlák B, Severijns N, Vanderpoorten W, Vanhaverbeke J, Vanneste L and Wouters J 1990 *Hyperfine Interact.* **59** 505–8

[16] Erzinkyan A L, Parfenova V P, Gurevich G M, Topalov S V, Shishkin D L, Finger M, Kapusta S, Pavlov V N and Slovák J 1990 *Hyperfine Interact.* **59** 457–60
[17] Flouquet J, Taurian O, Sanchez J, Chapellier M and Tholence J L 1977 *Phys. Rev. Lett.* **38** 81–4
[18] Coey J M D 1978 *J. Appl. Phys.* **49** 1646–52
[19] Kiymac K 1985 *Phys. Status Solidi* b **128** 553–62
[20] Hamzic A, Senoussi S and Campbell I A 1980 *J. Phys. F: Met. Phys.* **10** L165–9
[21] Hamzic A, Senoussi S, Campbell I A and Fert A 1980 *J. Magn. Magn. Mater.* **15–8** 921–2
[22] Erzinkyan A L, Parfenova V P, Reiman S I, Gurevich G M, Topalov S V and Shishkin D L 1991 *Sov. Phys.-JETP* **73** 720–4
[23] Le Dang Khoi, Veillet P and Campbell I A 1976 *J. Phys. F: Met. Phys.* **6** L197–200
[24] Kohgi M and Ishikawa Y 1980 *J. Phys. Soc. Japan* **49** 985–93
[25] Krén E, Kádár G, Pál L, Sólyom J, Szabó P and Tarnóczi T 1968 *Phys. Rev.* **171** 574–85
[26] Star W M, Foner S and McNiff E J 1975 *Phys. Rev.* B **12** 2690–709